

# TCAD for gate stack optimization in pGaN Gate HEMT devices

M.-A. Jaud, Y. Baines, M. Charles, E. Morvan, P. Scheiblin, A. Torres, M. Plissonnier and J.-C. Barbé  
Univ. Grenoble Alpes, F-38000 Grenoble France  
CEA, LETI, MINATEC Campus, F-38054 Grenoble France  
marie-anne.jaud@cea.fr

**Abstract**—pGaN Gate HEMTs are promising normally-OFF transistors for which the use of magnesium (Mg) doping allows the modulation of the threshold voltage ( $V_{th}$ ) but at the cost of an ON-state resistance ( $R_{on}$ ) degradation. In this study, we propose rigorous TCAD simulations that describe the Mg doping impact on both electrical parameters ( $V_{th}$  and  $R_{on}$ ) in agreement with experimental data. We emphasize the importance of TCAD as an additional tool to optimize this  $V_{th}$ - $R_{on}$  process-window

**Keywords**—pGaN Gate HEMT, Magnesium, TCAD

## I. INTRODUCTION

The AlGaN/GaN High Electron Mobility Transistor (HEMT) is an attractive structure for the realization of greener converters in multiple domains. With wide band gaps, high critical fields, the capability of high temperature operation, GaN and its alloys allow the emergence of power devices with aggressive scaling that enable high frequency power conversion. A specific feature of the HEMT structure is the presence of a two dimensional electron gas (2DEG) that naturally occurs at the AlGaN/GaN heterojunction and which presents a high carrier mobility combined to high carrier density [1-2]. Nonetheless, in virtue of the 2DEG induced by piezopolarisation, conventional HEMT are normally-on devices. Several architectures have been recently proposed to design normally-off GaN devices. Among them, Fluorine-implanted MIS-HEMTs allow to obtain positive threshold voltage [3]. Additionally, MOS-channel HEMTs have been studied to obtain accumulation of even inversion channels in the gate region [4]. Although these two structures have appealing features, they face the challenge of the fabrication of a robust and reliable MIS or MOS gate on a III-N heterojunction. In this paper, we propose to study the pGaN Gate HEMT that uses an epitaxial p-type gate material on the heterojunction to reach positive threshold voltage [5-7]. We first detail the principle of this architecture and the role of the p-type dopant. The main objective of this paper being the gate stack optimization of such a device by TCAD, we then describe how to introduce the Magnesium dopant in our simulations. We also present an in depth analysis of the incomplete ionization mechanism inherent to the Magnesium activation energy which is a deep acceptor. In the last part of this paper, the  $V_{th}$ - $R_{on}$  trade off evolution as a function of Magnesium doping, AlGaN thickness and AlGaN mole fraction is clearly exposed and explained. Finally TCAD is

confronted to experimental data and is shown to be in good agreement for various gate stacks.

## II. INTEREST OF MAGNESIUM FOR PGAN GATE HEMT

When an AlGaN layer is grown on a GaN layer, positive surface charges at the AlGaN/GaN heterointerface are created due to spontaneous and piezoelectric polarizations (in the case of Ga face orientated crystal). A triangular potential well with a two dimensional electron gas (2DEG) is induced to compensate this positive charge, making a conventional AlGaN-GaN HEMT normally-ON (Fig.1 black).

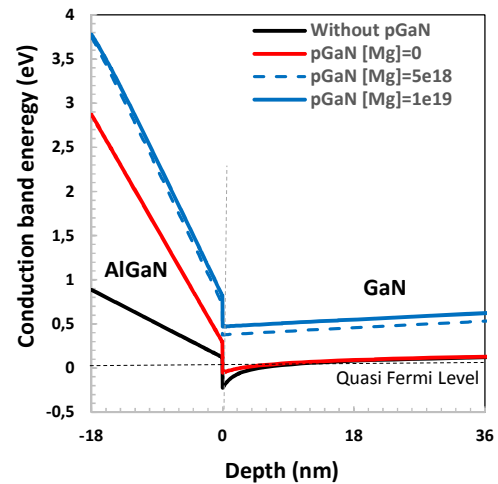


Fig. 1: Conduction band energy for an 18nm/18% AlGaN barrier and different pGaN configurations.  $V_g=0V$ . Schottky gate contact with  $W_f=4.5eV$ .

The pGaN Gate HEMT is an architecture that enables a normally-OFF device through the addition of a pGaN layer on the AlGaN barrier [5-7]. At the pGaN/AlGaN heterointerface, a negative polarization charge is created that shifts the conduction band upwards, thereby participating in the depletion of the underlying 2DEG (Fig.1 red). Moreover, Gallium Nitride possesses an important electron affinity (4.1 eV) which in combination to p-type doping and its wide band gap also lifts up the conduction band at the AlGaN/GaN interface (Fig.1 blue). From an integration point of view, it is common to grow the Mg doped pGaN layer over the whole wafer and form the gate post epitaxy [7-9]. This means that diffusion of Mg through the AlGaN barrier and the GaN

channel have to be considered over the entire device. The advantage of the use of Mg in the gate stack to modulate the  $V_{th}$  can therefore become a drawback in the access region and impact the Ron [8]. Through this study we show the importance of TCAD environments to optimize pGaN Gate HEMTs, in particular the need of a rigorous description of the Mg doping to address the  $V_{th}$ -Ron couple.

### III. MAGNESIUM SIMULATED PROFILE AND INCOMPLETE IONIZATION

The simulated pGaN Gate device is represented in Fig. 2, which also specifies its dimensions. It is considered as an ideal device with, for example, no sheet resistance degradation induced by pGaN etching in the access regions or ideal contact resistances. In the case of an 18nm/18% AlGaIn barrier capped with a pGaN layer containing an Mg dose of  $1.10^{19} \text{ cm}^{-3}$ , the TCAD Mg profile has been calibrated on an acquired Mg SIMS profile. Indeed, assuming that all the Mg atoms are on substitutional sites and that the activation annealing has removed all hydrogen passivation, SIMS can be used to describe TCAD Mg doping profiles (Fig. 3 red). Note that such profiles are described through an analytical expression that depends on the Mg dose and that the same analytical expression is used independently of the AlGaIn barrier (thickness and composition). It is illustrated in Fig. 3.

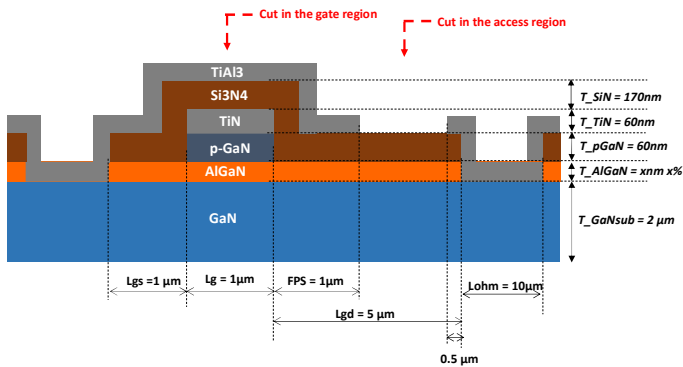


Fig. 2: Simulated device architecture

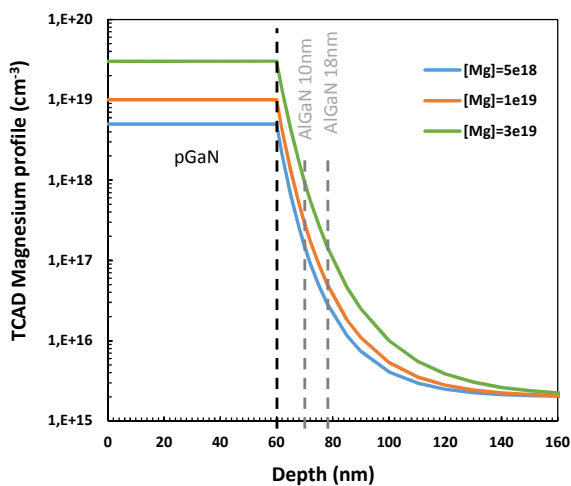


Fig. 3: TCAD doping Mg profiles for various Mg dose.

The Mg activation energy is assumed to be the same in GaN and AlGaIn with an acceptor state at 170meV from the valence band [7]. Because Mg is a relatively deep acceptor in III-N semiconductors, the incomplete ionization is taken into account through a Fermi-Dirac distribution as indicated in the following equation and illustrated in Fig. 4 in the case of acceptors [10].

$$N_A^- = \frac{N_{A,0}}{1 + g_A \exp\left(\frac{E_A - E_{Fermi}}{kT}\right)} \text{ for } N_{A,0} < N_{A,crit}$$

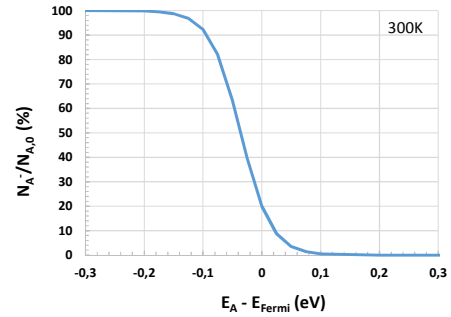


Fig. 4: Fermi-Dirac distribution describing the concentration of ionized impurity atoms ( $N_A^-$ ) in the case of acceptors with  $N_{A,0}$  the substitutional acceptor concentration,  $g_A$  the degeneracy factor for the impurity level,  $E_A$  the acceptor activation energy. Illustration: fraction of ionized dopant as a function of the Fermi energy ( $E_A=170\text{meV}$ ).

Fig 5 & 6 show band structures, simulated Mg doping profiles and calculated ionized Mg profiles for sections perpendicular to the electron transport in the access region and in the gate region at zero bias (sections are represented in Fig 2). In the access region (see Fig. 5), Mg dopants are fully ionized in the AlGaIn layer due to the built electric field, whereas in the GaN layer a compensation mechanism and low Mg concentration allows to account for, again, complete ionization. Note that the position of the Fermi level, close to the conduction band at the vicinity of the heterojunction, is in clear agreement with total ionization of acceptors ( $E_A - E_{Fermi} \ll 0$ ). In the gate stack (see Fig. 6), 4 regions can be distinguished: (i) close to the AlGaIn/GaN interface, the arguments raised previously apply the same way and full ionization is observed once again (ii) close to the pGaN/AlGaIn interface, where a negative polarization charge plane is present due to spontaneous and piezoelectric polarizations, one observes that the Fermi level drops to the valence band and Mg ionization becomes negligible ( $E_A - E_{Fermi} > 0$ ). At this interface, we see an accumulation of holes mainly coming from thermal generation from the valence band that compensates the negative polarization charge; (iii) at the metal/pGaN interface, the gate workfunction ( $Wf=4.5\text{eV}$ ) is lower than the pGaN workfunction, therefore electrons transit from the metal to the pGaN where they recombine with holes thus creating a depletion region at equilibrium. The resulting large electric field induces a complete ionization of Mg; (iv) in the middle of the pGaN layer, where the Fermi level is mainly influenced by p-doping, the Mg is partially ionized (about 4% for  $[Mg]=1.10^{19}\text{cm}^{-3}$  at 300K) with a concentration of holes equals to the Mg ionized concentration.

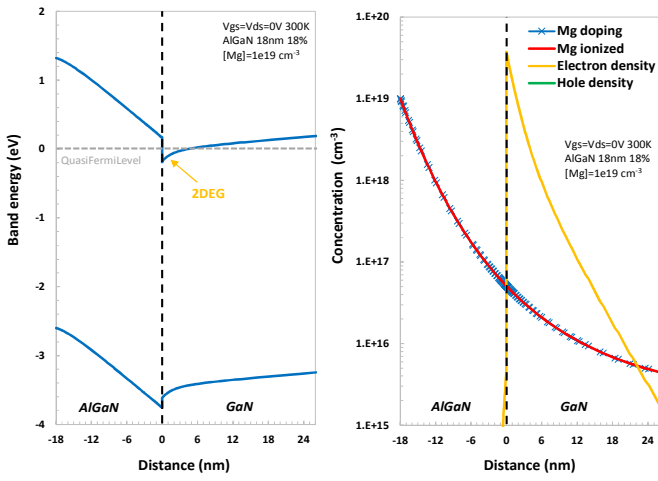


Fig. 5: Band structure, Mg doping, ionized Mg concentration, electron density and hole density extracted in the access region at  $V_{gs}=V_{ds}=0V$ .

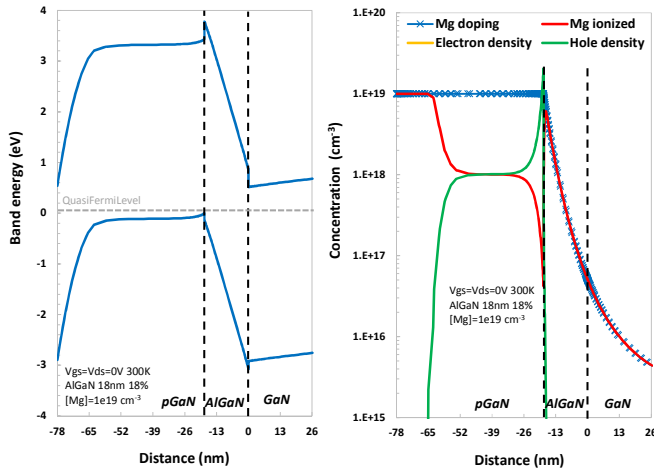


Fig. 6: Band structure, Mg doping, ionized Mg concentration, electron density and hole density extracted in the gate region at  $V_{gs}=V_{ds}=0V$ .

#### IV. V<sub>TH</sub>-RON TRADE-OFF

Electrical simulations were performed using Synopsys S-Device module [11]. The piezoelectric polarization strain model with Vurgaftman values [12] is used to take into account the piezo-polarisation effect. A mobility model including phonon scattering (with  $\mu_{max}=1500 \text{ cm}^2/(V.s)$  for electrons in GaN), doping dependent mobility degradation and high field saturation is assumed. Figure 7 show variations of electron density extracted from the access region ( $n_s$ ) as a function of  $V_{th}$ . Figure 8 show variations of  $R_{on}$  as a function of  $V_{th}$ . For these two figures a pGaN Gate HEMT with an 18nm thick AlGaN barrier containing 18% of Aluminum and a pGaN layer doped with an Mg dose of  $1.10^{19} \text{ cm}^{-3}$  is taken as reference. When the Aluminum content or the AlGaN thickness increase, the electron density ( $n_s$ ) at the AlGaN/GaN interface increases and therefore the  $R_{on}$  decreases. Consequently, it is more difficult for the gate to deplete the channel resulting in a  $V_{th}$  decrease. When the Mg dose increases, the conduction band is shifted upwards resulting in a decrease in  $n_s$  and an increase in  $R_{on}$  and  $V_{th}$ .

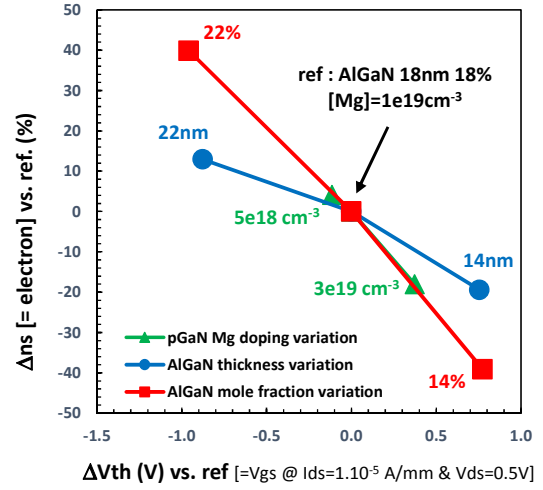


Fig. 7:  $n_s$  variations as a function of  $V_{th}$  for different AlGaN barrier thicknesses, AlGaN barrier compositions and Mg doses in the pGaN.

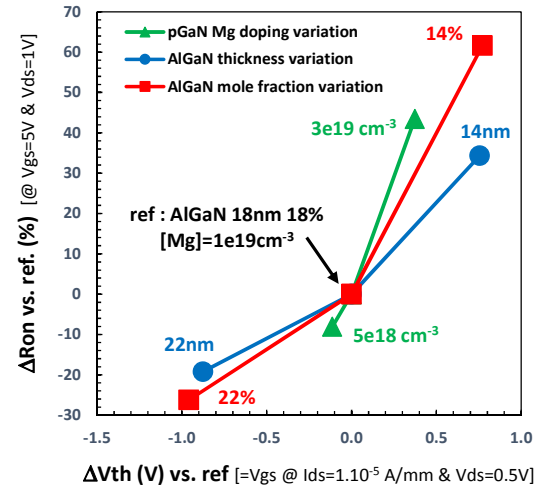


Fig. 8:  $R_{on}$  variations as a function of  $V_{th}$  for different AlGaN barrier thicknesses, AlGaN barrier compositions and Mg doses in the pGaN.

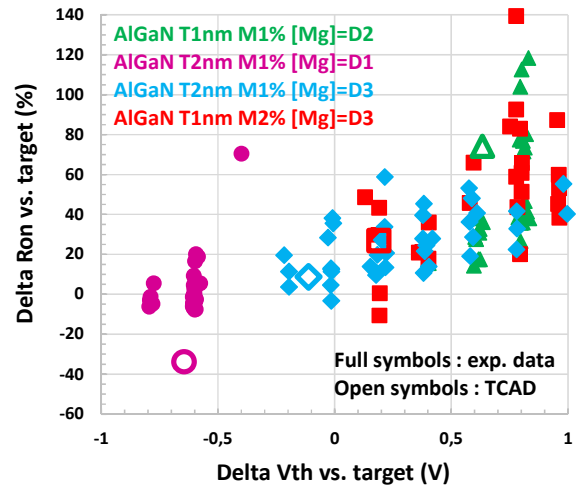


Fig. 9:  $\Delta R_{on}$  as a function of  $\Delta V_{th}$  for various AlGaN barrier thicknesses & compositions and Mg doses in the pGaN from TCAD and experimental data (ref. is our target in  $R_{on}$  &  $V_{th}$ ).

The  $\Delta V_{th}$ - $\Delta R_{on}$  trade-off obtained by TCAD simulations is compared with experimental measurements on Fig. 9. An overall good agreement is demonstrated. We thus validated the relevance of our TCAD approach for the simulation of the gate stack of a pGaN Gate HEMT in order to optimize the  $V_{th}$ - $R_{on}$  trade-off.

## V. CONCLUSION

In this study, TCAD simulation is proposed as an additional tool to optimize the gate stack of the pGaN-Gate HEMT in a  $V_{th}$ - $R_{on}$  trade off point of view. The Mg doping profile from the pGaN was introduced into a TCAD simulation by comparison with a representative SIMS profile. A rigorous investigation of the incomplete ionization of Mg is proposed through the analysis of the band structure in the gate stack and in the access regions. Clear explanations are given about the evolutions of the  $V_{th}$ - $R_{on}$  trade-off as a function of the Magnesium doping dose, the AlGaN thickness and the AlGaN aluminum mole fraction. Finally TCAD is shown to be consistent with experimental data obtained on various gate stacks. We show thereby the relevance of TCAD as a powerful and reliable tool to define an optimized process-window to address the trade-off between  $V_{th}$  and  $R_{on}$ .

## ACKNOWLEDGMENT

The authors kindly thank Ferdinando Iucolano from STMicroelectronics for fruitful discussions.

## REFERENCES

- [1] S. Mohammad *et al.*, "Emerging gallium nitride based devices", IEEE vol. 83, no. 10, pp. 1306-1355, 1995.
- [2] U. Mishra *et al.*, "AlGaIn/GaN HEMTs-an overview of device operation and applications", IEEE, vol. 90, no. 6, pp. 1022-1031, 2002.
- [3] K.J. Chan *et al.*, "Physics of fluorine plasma ion implantation for GaN normally-off HEMT technology", IEEE International Electron Device Meeting, pp. 465-468, 2011.
- [4] H. Kambayashi *et al.*, "Enhancement-mode GaN hybrid MOS-HFETs on Si substrates with over 70 A operation", in proceedings ISPSD, 2009.
- [5] Y. Uemeto *et al.*, "Gate injection transistor (GIT)-A normally-off AlGaIn/GaN power transistor using conductivity modulation", IEEE Transaction on Electron Devices, vol. 54, no. 12, pp. 3393-3399, 2007.
- [6] O. Hilt *et al.*, "Normally-off AlGaIn/GaN HFET with p-type GaN gate and AlGaIn buffer", in proceedings Int. Symp. Power. Semicond., pp. 347-350, 2010.
- [7] I. Hwang *et al.*, "1.6 kV, 2.9 mΩ cm<sup>2</sup> normally-off pG-GaN HEMT devices", in proceedings ISPSD, pp. 41-44, 2012.
- [8] N.E. Posthuma *et al.*, "Impact of Mg out-diffusion and activation on the p-GaN gate HEMT device performance", in proceedings ISPSD, 2016.
- [9] L.-Y. Shu *et al.*, "Enhancement-mode GaN-based High-Electron mobility transistor on the Si substrate with a p-type GaN cap layer", IEEE Transaction on Electron Devices, vol. 61, no. 2, pp. 460-465, 2014.
- [10] S. M. Sze *et al.*, Physics of semiconductor devices, Third edition, p.22.
- [11] Synopsys, TCAD tool, SDevice User Guide L-2013.03, p. 886.
- [12] I. Vurgaftmann *et al.*, "Band parameters for nitrogen-containing semiconductors", Journal of Applied Physics, vol. 94, p. 3675, 2003.